Thermal Expansions from 2 to 40°K of Ge, Si, and Four III-V Compounds*

P. W. SPARKS† AND C. A. SWENSON
Institute for Atomic Research and Department of Physics, Iowa State University, Ames, Iowa
(Received 16 June 1967)

Linear thermal-expansion data are given for Ge, Si, GaAs, GaSb, InAs, and InSb at temperatures from 1.89°K to approximately 40°K. The data were obtained using a variable transformer as a sensor and are absolute in sample length changes. At the lowest temperatures, the length-change data for 10-cm samples exhibit a scatter of ± 0.02 Å (or $\pm 2\times 10^{-11}$ in $\Delta L/L_0$). The precision at all temperatures (within this limitation) is 2%. All of these substances show a positive thermal-expansion coefficient which is proportional to T^3 at low temperatures, while at higher temperatures the expansion coefficient becomes negative. The linear thermal-expansion data are used to calculate the temperature dependence of the Grüneisen constants for each of these. With the exception of Si, a correlation exists between the Debye temperature and both the magnitude of γ_0 and the shape of the γ-versus-T curve. There is discrepancy between our observed values of γ_0 for Ge and Si (0.66 and 0.42, respectively) and those calculated from the 77°K third-order elastic-constant data. The reason for the discrepancy (which is a factor of 2 for Si) is not known.

I. INTRODUCTION

A COMMON characteristic of tetrahedrally bonded solids appears to be the existence of a region of a negative thermal-expansion coefficient below a reduced temperature of approximately $T/\Theta_D=0.2$ (where Θ_D is a Debye temperature). Gibbons[1] reported this behavior in Si and InSb at temperatures down to 4°K, while Novikova has reported similar results for Ge, Si, GaAs, GaSb, α-Sn, diamond, ZnSe, etc.[2] Barron[3] and Blackman[4] have shown that it is possible to understand these negative expansion coefficients in terms of instabilities in the low-lying transverse acoustic modes of the phonon distribution.

Daniels,[5] however, pointed out that the then existing data for the pressure dependence of the elastic constants for Ge and Si could be used to predict a small positive thermal-expansion coefficient for these materials at the lowest temperatures. This prediction was experimentally verified by White and his co-workers,[6,7] who showed that the thermal expansions of germanium and silicon indeed became positive below reduced temperatures $T/\Theta\sim 0.04$. The sensitivity of their capacitive technique was not sufficient to establish precisely the magnitude of this expansion for comparison with the high-pressure elastic results, however.

The objective of the work described in this paper was twofold. First, we hoped to establish the magnitudes of the low-temperature thermal expansions of Ge and Si with sufficient precision to make a quantitative comparison with Daniels's predictions. Second, we planned to investigate the thermal expansions of several other related tetrahedrally bonded solids (the III–V compounds GaAs, GaSb, InAs, and InSb) for similar behavior and to attempt to establish correlations which would help to understand this class of solids. No basic theory exists for these solids although shell-model calculations by Dolling and Cowley[8] have shown that the thermodynamic properties of Si, Ge, GaAs, and diamond (including the thermal expansion) can be understood in terms of the lattice dispersion curves as determined by inelastic neutron scattering.

The magnitudes of the linear thermal expansions of these materials are of the order of 10^{-10} °K^{-1} at the lowest temperatures. Hence, their direct measurement involves the detection of 0.1 Å changes in length for 10-cm-long samples. We have been able to determine thermally induced length changes with a sensitivity of ± 0.02 Å (and a precision of approximately 2%) for 10-cm-long samples using a refinement of the mutual inductance technique developed by Carr and Swenson.[9] The basic method which was used as well as data which were obtained for Ge, Si, and four III–V compounds from 2 to 40°K are described below.

II. EXPERIMENTAL DETAILS

The basic technique which was used for these measurements is the same as that described by Carr and Swenson.[9] One end of a relatively long sample is coupled mechanically to the movable secondary of a variable transformer. The top and bottom halves of

* Work was performed in the Ames Laboratory of the U. S. Atomic Energy Commission. Contribution No. 2081.
† Lt., U. S. Navy. Present address: U. S. Naval Nuclear Power Training Unit, West Milton Site, Schenectady, N. Y.
[1] D. F. Gibbons, Phys. Rev. **112**, 136 (1958).
[2] S. I. Novikova, in *Physics of III-V Compounds*, edited by R. K. Willardson and A. C. Beer (Academic Press Inc., New York, 1966), Vol. 2, p. 33. This paper gives a summary of thermal-expansion work on III-V compounds and a discussion of the author's work.
[3] T. H. K. Barron, Ann. Phys. (N. Y.) **1**, 77 (1957).
[4] M. Blackman, Phil. Mag. **3**, 831 (1958).
[5] W. B. Daniels, Phys. Rev. Letters **8**, 3 (1962); in *Proceedings of the International Conference on Semiconductors, Exeter* (The Institute of Physics and the Physical Society, London, 1962), p. 482.
[6] R. D. McCammon and G. K. White, Phys. Rev. Letters **10**, 234 (1963).
[7] R. H. Carr, R. D. McCammon, and G. K. White, Phil. Mag. **12**, 157 (1965). This paper gives an excellent review of previous work on Ge and Si.
[8] G. Dolling and R. A. Cowley, Proc. Phys. Soc. London **88**, 463 (1966).
[9] R. H. Carr and C. A. Swenson, Cryogenics **4**, 76 (1964).

this secondary are wound in opposite directions, and for small motions about a null position (of the order of ± 1 mm) the coupling between the primary and secondary (as measured with a mutual inductance bridge) is a linear function of the secondary motion. The resulting sensitivities (less than 10^{-9} cm) are comparable with or better than can be obtained with other techniques.[10] In addition, the linearity of the device for large (mm) motions and its capability for detecting absolute length changes are decided advantages. The earlier design was modified for the present work with the secondary placed in the same vacuum chamber as the sample. This simplifies the problem of transferring sample motion to the secondary but introduces problems of thermally anchoring the secondary to the surrounding liquid-helium bath.

A cutaway sketch of the apparatus is shown in Fig. 1. The sample (which is usually 10 cm long and between 6 and 8 mm diameter) drives the secondary by means of the thin fused-quartz spacer (2 cm long). The secondary support, which allows only longitudinal motion, is not shown. The temperature of the sample is changed by passing a current through the 40-Ω heater, and temperature differences between the sample and the surrounding liquid-helium bath are measured by means of a Au-Fe–versus–Cu differential thermocouple.[11] The leads from the hot junction of the thermocouple, as well as the heater and secondary leads, pass continuously through the connector shown in Fig. 1.

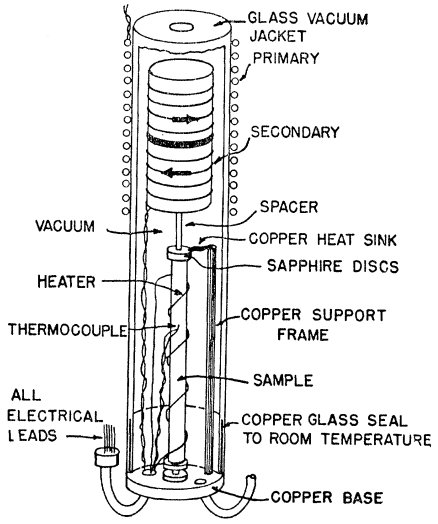

FIG. 1. A sketch of the thermal-expansion cell. The surrounding liquid-helium and liquid-nitrogen Dewars are not shown. The continuous-lead electrical pass-through shown consists of a nylon cap, epoxied to a stainless steel tube, with electrical leads also epoxied into a hole or series of holes in the cap. Care must be taken to use epoxies as recommended by the manufacturer and not to use cotton or silk-covered wire.

[10] J. G. Collins and G. K. White, in *Progress in Low Temperature Physics*, edited by C. J. Gorter (North-Holland Publishing Company, Amsterdam, 1964), Vol. 4, p. 450.

[11] R. Berman, J. C. F. Brock, and D. J. Huntley, Cryogenics 4, 233 (1964).

The heat flow through the ends of the sample is limited by sapphire disk thermal "breaks." These make use of the relatively high thermal impedance which exists between two smooth, hard surfaces in a vacuum.[12] Sapphire disks are glued to each end of the sample and also to heat sinks at the top and bottom of the sample chamber. The lower disks are indented and a sapphire ball (see Fig. 1) is placed between them to act as a gimbal bearing. The upper two sapphire disks are held in close contact by the weight of the secondary as transmitted by the spacer. The upper heat sink is a copper foil which is anchored directly to a copper rod which terminates in the liquid-helium bath. Sideways motion of the sample is prevented by three horizontal nylon strings which are spring-loaded to maintain tension and which are anchored to the frame. Typically, a power of approximately 35 mW applied to the sample is sufficient to produce a sample temperature of 25°K. The vacuum chamber is connected by means of a small pumping line to a valve and a pressure relief valve at room temperature. It is pumped with a forepump before a run and then sealed off before liquid helium is transferred.

Two major problems involve thermal anchoring, to ensure that only the sample changes temperature, and vibration elimination. The thermal anchoring of both the secondary and the spacer is made directly to the helium bath by means of fine copper wires attached to copper posts (not shown). An unexpected source of heating in the secondary is due to eddy currents generated by the 30-G (rms), 250-cps primary field. This heating is one or two orders of magnitude greater than had been expected and is most likely due to interwinding capacitance effects. This heat is removed by means of copper strips inserted between the windings and anchored to the bath as mentioned above. In operation, even with this anchoring, supplementary measurements showed that the secondary temperature floats two or three degrees above the bath. This temperature difference is constant, however, independent of sample power input and is not important.

The vibration problems involve boiling in both the liquid-nitrogen and liquid-helium Dewars, and the transfer of building noise. The latter is eliminated by resting the Dewar head support on two horizontal inflated automobile tire inner tubes which lie on a platform attached to a wall. This elementary suspension is extremely successful, probably in part because of the large mass of the Dewars plus liquid nitrogen (roughly 200 lb). To prevent bubbling, the liquid helium is pumped and regulated at a temperature below the λ point (1.89°K) while the liquid nitrogen is pumped to the triple point and then sealed off.

The details of the various portions of the measurement system are given below together with a brief discussion of the difficulties encountered. The measure-

[12] R. Berman and C. F. Mate, Nature, **182**, 1661 (1958).

ments are not routine, and internal checks (which will be discussed in Sec. III) are needed to verify the reliability of the data obtained.

A. Variable Transformer

The variable transformer is an air-core device which consists of independent primary and secondary coils. As is indicated in Fig. 1, the secondary coil (3.2 in. long, 1.0 in. o.d.) consists of two halves which are wound in opposite directions. Each half contains 5000 turns of No. 38 copper wire. The coil is free-standing (no core material is involved) and is bonded together using G. E. 7031 varnish.[13] At 4°K, the resistance and inductance of the coil are 21 Ω and 0.4 H, respectively. To reduce effects due to the thermal expansion of the secondary, it is driven by the quartz spacer from a point which is at the geometrical center of the coil. Every attempt is made to retain symmetry. Longitudinal copper strips which were made an integral part of the coil serve both to cool the coil initially and to remove eddy-current heating. The secondary is suspended from a glass-impregnated phenolic frame by six nylon strings (three on each end) which allow only longitudinal motion.

The primary coil is designed to reduce coupling with the secondary which could occur via nearby conductors (eddy currents), magnetic materials, etc. It is wound on a glass-impregnated phenolic form with a winding inside diameter of approximately 1.8 in. It can be moved easily on the glass vacuum jacket for rough adjustment at room temperature before being fixed in place. It is immersed in liquid helium in actual operation. The center section of the primary (2500 turns of No. 32 copper wire) is 1.5 in. long and is wound in a clockwise direction. The two equivalent end sections (one on each end of the center, and each 0.75 in. long and containing 1250 turns) are wound in the opposite direction to produce roughly zero net magnetic moment for the primary when viewed from a distance. The resistance and inductance of this coil at 4°K are 10 Ω and 3.6 H, respectively. The field configuration (at 100-mA current) is roughly a maximum of +30 G at the center, and −12 G one-half secondary length from the center.

The above data can be used to estimate the sensitivity of this coil system about null as 3×10^{-8} V/Å for a 250-cps, 100-mA primary current. Off-null voltages of approximately 10^{-10} V can be detected electrically using a good transformer and a phase-sensitive detector so the estimated sensitivity can be well below 0.1 Å.

B. Mutual-Inductance Bridge

In the earlier work[9] a conventional Hartshorn bridge was used to measure the changes in coupling. These bridges suffer from a lack of stability and a limited range. Following the suggestion of Dr. A. M. Thompson of the National Standards Laboratory, Sydney, Australia,[14] we replaced the earlier bridge with the circuit shown in Fig. 2, which is similar to the bridge described by Maxwell.[15]

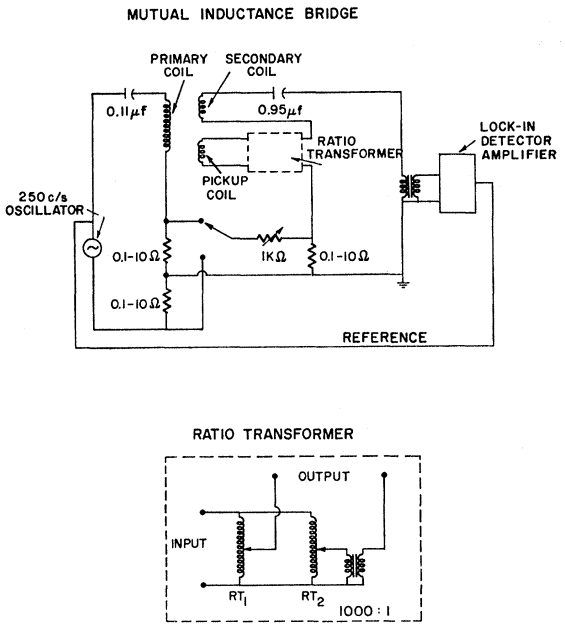

FIG. 2. The mutual-inductance bridge used in this work. The primary, secondary, and pickup all are located at 1.89°K, the rest of the apparatus is at room temperature.

The heart of the bridge is a combination of Gertsch Model 1011 R ratio transformers. These instruments essentially are high-quality auto-transformers which have an open-secondary input impedance of 300 000 Ω at 250 cps, a least count of 10^{-7} and a linearity of 10^{-6}. The "pick up" coil shown in Fig. 2 serves to produce a fixed, stable coupling to the primary which is subdivided by the ratio transformers. It contains 1000 turns, has a resistance of 6.5 Ω at 4°K, and is wound directly on the various sections of the primary (matching turn directions).

The resistance network (Fig. 2) is used to balance the out-of-phase signals while the two capacitances are used to tune both the primary and the secondary circuits to make their impedance purely resistive. The transformer is a 10^3:1 high-quality geophysical type which somewhat overmatches the secondary impedance into the input of the locally designed phase-sensitive detector.[16] The oscillator is an Optimation Model AC15, which provides extreme stability (0.01%) in both frequency and amplitude for the bridge current.

One of the major attractive features of the variable

[13] We have found that the new "Nyclad" insulated copper wire sold by the Belden Wire Corporation is not attacked by the normal solution of this varnish in methanol and toluene. This was not true of earlier versions of "Nyclad."

[14] A. M. Thompson (private communication) transmitted by R. H. Carr. The authors are indebted to Dr. Thompson and Dr. Carr for their correspondence on this subject.

[15] E. Maxwell, Rev. Sci. Instr. 36, 553 (1965).

[16] W. A. Rhinehart and L. Mourlam, U. S. Atomic Energy Commission Report No. IS-821, 1964 (unpublished).

transformer is that it can be designed so as to give a linear response for relatively large ranges of motion (±1 mm). Hence, we planned to calibrate the ratio transformer settings versus displacement directly using a micrometer slide (reading to 10^{-4} cm) to measure the motion of the secondary with respect to the primary. The pickup coil was designed to cover this range, but a least count of 10^{-10} also was required for bridge balances at the sub−0.1 Å level. The ratio transformers are limited to seven decades so the range was extended using a second ratio transformer (RT-2 in Fig. 2), the output level of which was reduced by 1000 using the step-down transformer shown. In practice, rough balances (and all calibrations) are done using RT-1 while a typical thermal-expansion measurement involves only variations in RT-2 settings.

With this arrangement we are able to detect changes in the coupling between the primary and secondary of the order of 10^{-11}. Once the variable transformer has been cooled to 1.9°K the stability is of this same order of magnitude. The major limitation at the moment appears to be associated with residual vibration and electrical building noise.

C. Calibration Procedures

The bridge-variable transformer combination was calibrated versus the micrometer slide (Gaertner, 5.0-cm range), and a linearity of ±0.3% was found over a range of ±1 mm. Because of the purely geometrical nature of the coupling and the care taken in the choice of nonmagnetic construction materials, we find very little (less than 1%) variation in the calibration upon going from room temperature to 4°K. The linearly extrapolated full ratio transformer range (if usable) would correspond to 1.130 (±0.003) cm, giving a least count of 0.011 Å. In practice, all calibrations are carried out with the variable transformer immersed in liquid nitrogen in order to reduce the resistance of the coils. Checks with other thermal-expansion data justify our assumption that the linearity of the calibration extends to the Angstrom level. Care must be taken in the choice of the portion of the variable-transformer range which is used since the region near zero mutual inductance shows nonlinear behavior, and one side of the null position usually has a more linear calibration than the other. Hence, data are taken midway in a calibrated region.

D. Thermometry

The temperature scale used in these measurements is based on the use of Au+0.07 at.%Fe–versus–Cu thermocouples.[11] A preliminary calibration of the wire we used has been reported in terms of constant-volume gas-thermometer temperatures to 20°K,[17] and these early data have been supplemented by precise comparisons both with more recent constant-volume gas-thermometer data and platinum resistance thermometers calibrated at the National Bureau of Standards on the NBS 1955 scale.[18] The various temperatures are believed to be reliable to ±0.02°K and the values of the thermoelectric power dE/dT correct to at least 0.5%.

The thermocouples are used in a differential manner to measure the temperature difference between the sample and the surrounding helium bath, with copper leads extending to room temperature. The bath temperature is maintained constant at 1.89°K using a giant manostat to regulate the vapor pressure.[9] The thermocouple itself is wound about the sample several times and is glued with G. E. 7031 varnish at several places to provide thermal anchoring. The thermocouple leads are continuous through the seal shown in Fig. 1, and the bath junction is immersed directly in liquid helium.

The thermoelectric power of the thermocouples is 11 μV/deg at both 4 and 40°K, with a maximum value of 14 μV/deg at 15°K. The total emf at 40°K (with respect to 1.89°K) is of the order of 450 μV. Our requirements basically involve observing temperature differences to 10^{-3} °K (or emf changes of 0.01 μV) although the precision in absolute temperatures need be only 0.1%. This is done in a manner which is essentially potentiometric, with a Keithley model 150-A microvoltmeter being used both as a null detector and as a microvoltmeter for the direct determination of small temperature changes. The magnitudes of the stray thermal emf's in the circuit are determined from readings taken with zero power into the heater, and these values (usually of the order of 2 μV) are checked periodically during a run.

E. Technical Problems

The major problem involved in the design of the low-temperature portions of the expansion apparatus (Fig. 1) is to ensure that only the sample changes temperature when current is applied to the heater. Hence, extreme care is taken with respect to thermal "grounding" of all components directly to the helium bath. Temperature changes can manifest themselves in two ways: first, as undesired length changes, and second, as changes in either electrical or magnetic properties of construction materials which will be reflected via changes in the primary-secondary coupling as apparent length changes. Hence, only the highest-purity copper is used in the thermal grounding system, no magnetic material (such as stainless steel, Constantan, etc.) is used in the construction of the cell, and only nonsuperconducting silver solder or Cd-Bi soft solder is used to make connections. The use of fused quartz in the push-rod assembly was dictated by the

[17] D. K. Finnemore, J. E. Ostenson, and T. F. Stromberg, U. S. Atomic Energy Commission Report No. IS-1046, 1964 (unpublished).

[18] M. S. Anderson and C. A. Swenson (unpublished).

basically nonmagnetic nature of this solid, not by its thermal expansion (which is relatively large and negative at these temperatures).[19] Similarly, we use a glass Dewar system in place of the previous metal system[9] to eliminate the slow drifts in bridge balance which were observed and which were due presumably to variations in the temperature distribution of the metal and corresponding changes in its electrical resistivity. Pyrex glass is used for the vacuum jacket and a glass-impregnated phenolic is used for the primary coil form, since these both are immersed in liquid helium and are kept at constant temperature.

One additional complication arises when even slightly ferromagnetic materials (such as 300-series stainless steel) are present near the variable transformer. The field-dependent susceptibility of these materials makes the balance of the bridge current-dependent, and small fluctuations in the primary current appear as noise in the output due to fluctuations in the balance point. Every effort is made to keep the Au-Fe–versus–Cu thermocouples away from the variable transformer since even the small (0.07 at. %) iron concentrations can cause difficulty. It is obvious from the above that it would be difficult to study with this apparatus magnetic or superconducting materials. Metals which show a great variation in electrical resistivity with temperature also could cause trouble due to temperature-dependent eddy-current effects. To minimize these effects we have made one sample holder quite long so that the quartz spacer can be increased to 2 or 3 in. in length for 3-in.-long samples.

Another purely electrical problem involves the location of electrical grounds. In our apparatus, one side of the input to the phase-sensitive detector-amplifier is made the only system ground. Great care is taken to prevent ground loops through shielding, chassis grounds, etc. These precautions are obvious to anyone who has worked with low-level signals although the existence of problems is not always obvious.

F. Experimental Procedures

The sample and sapphire disks are cleaned with a solvent such as acetone to remove all grease, and the heater (wound astatically) and thermocouple, along with the two end sapphire disks, are attached to the sample with G. E. 7031 varnish. Spotlessly clean sapphire surfaces are essential for good thermal impedance. The sample is placed in the cell (Fig. 1), transverse nylon tie strips are attached from it to the frame (not shown), and the upper heat sink is arranged in place. The quartz spacer is adjusted to approximately the proper length (a bit short for these samples which contract less than copper on cooling) and is placed in position so that the secondary weight holds the upper heat sink in contact with the end of the sample. The copper bottom of the glass outervacuum jacket then is sealed in place with Wood's metal and the sample holder is evacuated to approximately 10^{-3} Torr before the valve which remains at room temperature is sealed off and the backing pump disconnected.

The primary is placed on the outside of the jacket and its position is adjusted so that its relative position with respect to the secondary will be about 0.3 mm from the zero mutual-inductance position when the system is cooled to 4°K. This can be done only by empirical methods.

The cell is placed in the helium Dewar and precooling to 77°K is started by placing liquid nitrogen in the nitrogen Dewar with a slight amount of nitrogen gas in the helium Dewar vacuum space. Heat is added to the sample at 77°K to verify that the thermocouple and mutual inductance systems are working properly; the thermal impedance of the sapphire thermal "breaks" is quite small here so quite large currents are necessary. Finally, liquid helium is added to the Dewar, and the cell is cooled to 4°K. This cooling requires several hours since the connection of the secondary to the bath via its thermal "grounds" is quite poor. An initial fill of roughly 14 liters of helium is adequate to cool the secondary to 4°K and then to run for 10 h at 1.89°K.

Final systems checks are made again at 4°K to verify that all is well. In particular, the mutual inductance must follow the sample temperature changes closely and the temperature must follow heater current changes with a reasonable time constant. The approximate heater current necessary to produce a given temperature is known from previous runs as well as the time constant with which the sample cools when the heater current is interrupted. These time constants (in which the temperature of the sample decreases to roughly half its value) vary from a minute or so for small-heat-capacity samples (like silicon) to 10 min or so for a large-heat-capacity sample like InSb. If all of these checks are positive, the liquid helium is pumped down to 1.89°K and its pressure is regulated. If the time constant remains the same as at 4°K, it may be concluded that no super-leaks exist in the system. In the event that a low-temperature leak should develop, a pressure relief valve (or vacuum pop-off) at room temperature prevents the build-up of excess pressure when the cell is removed from the Dewar.

Two quite different methods are used to obtain thermal-expansion data. At low temperatures where length changes are small (less than 8°K), direct readings are taken of the mutual-inductance changes as a function of temperature. These are fitted to an analytic function where possible, and thermal-expansion coefficients are calculated from this function by differentiation. Frequent checks are made to ascertain that irreversible "changes" of length have not occurred by decreasing the temperature to a previous value. These zero changes could be due to vibration, electrical pickup, or to friction effects in the sapphire spacers.

[19] G. K. White, Cryogenics 4, 2 (1964).

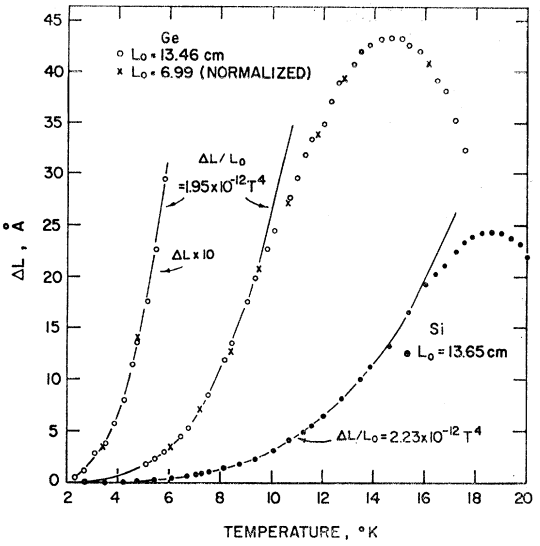

FIG. 3. The low-temperature thermal expansions of Ge and Si. The two Ge samples are from the same piece, and the data for the shorter sample have been normalized by multiplying the length changes by (13.46/6.99) so that the "long" and "short" sample data can be compared on the same scale. The Ge data plotted in the left-hand curve have been multiplied by a factor of 10 for display purposes.

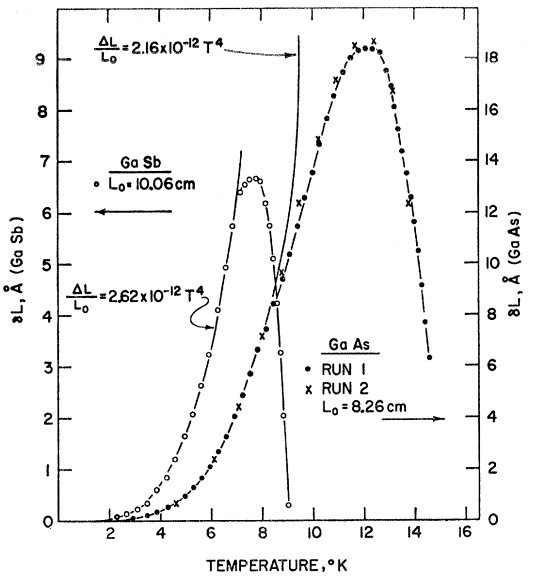

FIG. 5. The low-temperature thermal expansions of GaSb and GaAs. The GaAs sample was removed from the sample holder between runs 1 and 2.

These data essentially consist of a series of ΔL readings as a function of temperature.

At high temperatures, a procedure can be used which is similar to that used for heat-capacity measurements. Here the length change ΔL is measured for a relatively small temperature change ΔT (where ΔT is of the order of $0.1T$ or 1°K, whichever is smaller), and an average thermal-expansion coefficient is defined as $\alpha = L^{-1}\Delta L/\Delta T$. The thermoelectric power dE/dT of the thermocouples is used directly here. These data then consist of a series of direct determinations of α as a function of temperature. We have one advantage over the heat-capacity measurements in that the sample can be cooled back to its original temperature and the resulting negative length change determined. This gives an excellent check for friction or extraneous vibration effects. In general, the thermal-expansion coefficients as well as the total length changes from 1.89°K to a given temperature are recorded. The maximum temperature at which data are taken (approximately 40°K) is limited by an uneasy feeling that the necessarily large heat flows are causing temperature gradients in the sample.

In general, a check is made in each series of runs for effects due to a lack of temperature homogeneity in

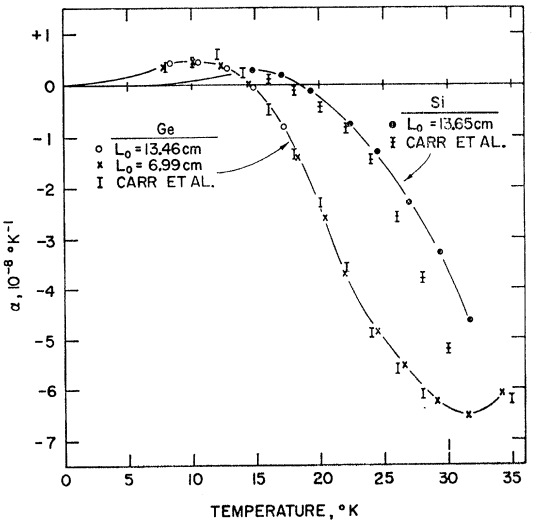

FIG. 4. "High"-temperature linear-thermal-expansion-coefficient data for Ge and Si. The data for Carr, McCammon, and White (Ref. 7) are shown also.

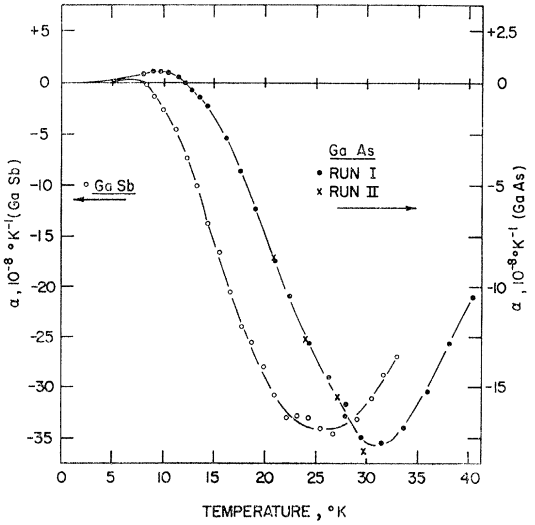

FIG. 6. The "high"-temperature linear-thermal-expansion coefficients for GaSb and GaAs. The GaAs sample was removed from the sample holder between runs 1 and 2.

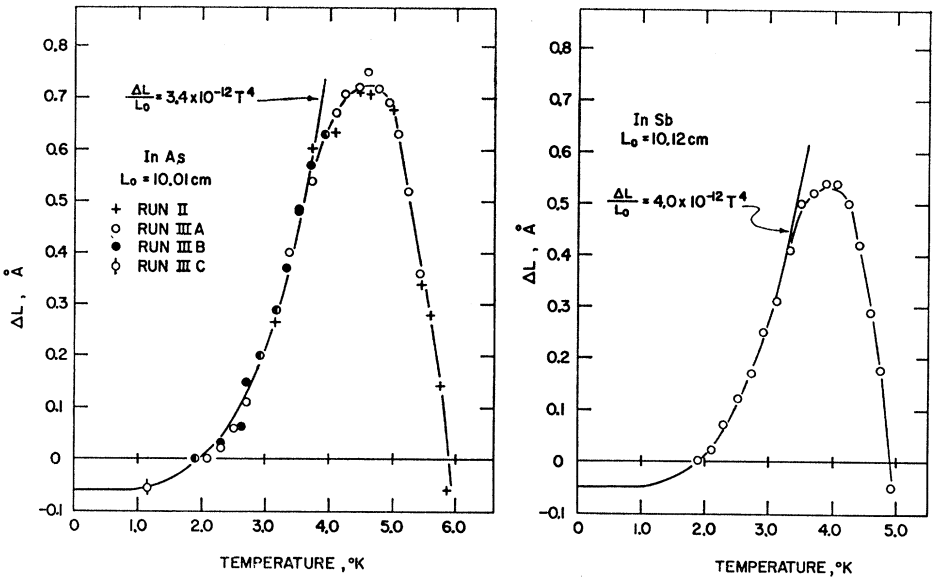

FIG. 7. The low-temperature expansions for InSb and InAs. The various runs for InAs were made on different days in the same setup. Run III-C was made from a bath temperature of approximately 1.15°K rather than the normal 1.89°K.

the sample. A basic assumption of our method is that the temperature of the sample is uniform and that all of the temperature difference between the sample and the bath appears across the interfaces between the sapphire disks. To be able to verify this, the heater always is wound in two sections, one on the top half of the sample and the other on the bottom half. Data normally are taken with the same current flowing through both halves of the heater, producing a uniform heating. But data also can be taken with current flowing through only, say, the heater on the top half of the sample, introducing a deliberate heating asymmetry. These checks were made periodically in the course of taking the data described in the following section, and no effects were observed which could be ascribed to poor thermal conductivity of the sample.

G. Sample Details

The physical and electrical characteristics of the samples which were used in these measurements are given in Table I. The samples were ordered as single crystals, but no check was made to verify that they actually were not polycrystalline. The estimates of carrier concentration (in most cases based on the resistivity)[20] were made in order to provide reassurance that free-carrier effects were not being observed.[21,22]

III. RESULTS AND CALCULATIONS

A. Experimental Results

The experimental data for the six semiconductors which we studied are given in Figs. 3–8, and smoothed thermal-expansion data are listed in Tables II and III. All of the ΔL data (Figs. 3, 5, 7) could be represented by a T^4 dependence within the scatter of the data at sufficiently low temperatures ($T/\Theta<0.02$), and the appropriate relationships are indicated on the figures. The resulting expression for the linear-thermal-expansion coefficient α and the maximum temperature to which it applies are given in Tables II and III.

The behavior of all of these solids above the T^4 region is similar in that the thermal-expansion coefficient rapidly becomes large and negative. Certain regularities (such as a correlation with the Debye temperature) will be discussed in a later section. Specific details of measurements on the various samples are given below, with a comparison with previous data. In gen-

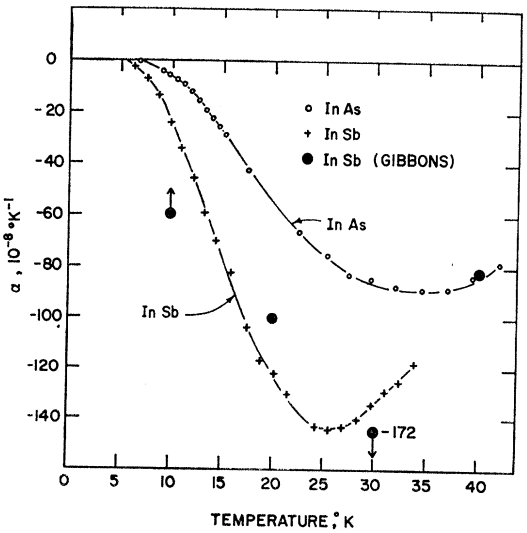

FIG. 8. The "high"-temperature linear-thermal-expansion coefficients for InAs and InSb. The early data of Gibbons (Ref. 1) are shown for comparison with our InSb data.

[20] N. B. Hannay, *Semiconductors* (Reinhold Publishing Corporation, New York, 1959).
[21] J. R. Drabble and J. Fendley, J. Phys. Chem. Solids **28**, 669 (1967).
[22] S. I. Novikova, Fiz. Tverd, Tela **7**, 2493 (1965) [English transl.: Soviet Phys.—Solid State **7**, 2007 (1966)].

TABLE I. Summary of the electrical and physical characteristics of the samples which were used in this investigation, together with the source of the crystal.

Sample	4°K Length (cm)	Average diameter (cm)	Resistivity 300°K (Ω cm)	Net carrier concentration[a] (cm^{-3})	Source
Si	13.65	0.9	150	$\sim 10^{15}$	Texas Instr.
Ge	13.46	1.2	48	$<10^{17}$	Mono-Silicon
	6.99				
GaAs	8.26	0.6	0.002	$\sim 2\times10^{18}$	Texas Instr.
GaSb	10.06	0.6	0.68	$\sim 10^{17}$	Texas Instr.
InAs	10.01	0.6	0.012	$\sim 2\times10^{16}$	Texas Instr.
InSb	10.12	1.0	0.024	$<2\times10^{16}$	Ohio Semi-conductors

[a] The various uncompensated impurity concentrations were determined by comparing the observed resistivities with those of doped samples. Data for Ge, Si, GaSb, and InSb were obtained from Ref. 20, while the data for GaAs and InAs were obtained from unpublished literature supplied by Texas Instruments. In addition, the reflectivities of Ge and Si as measured by D. W. Lynch of this laboratory indicated an impurity concentration of less than 5×10^{17} cm^{-3}. The sample purity for InSb was substantiated by helicon dispersion relations which were observed in a piece of this sample by J. L. Stanford of this laboratory.

eral, the data of Novikova[2] do not have sufficient precision in the region where they overlap ours to make any significant comparison.

1. Ge and Si

The only existing low-temperature data with which we can compare our results are those of Carr, McCammon, and White[7] for Ge and Si. The comparison of these data and our data is indicated in Fig. 4 where the error bars indicate the limits of uncertainty of the smoothed values given in Ref. 7 ($\pm10^{-8}$ °K^{-1}). The agreement between the two sets of Ge data is excellent, as is the agreement between the Si data up to 25°K. The origin of the deviations between the two sets of Si data above 25°K is not known but could be due to an unsuspected error in our measurements on this sample. Our data were obtained in a single run.

TABLE II. Smoothed values for the linear-thermal-expansion coefficient α and Grüneisen constant γ for Si and Ge.

	Si[a]		Ge[b]	
T (°K)	α (10^{-8} °K^{-1})	γ	α (10^{-8} °K^{-1})	γ
0	0	$0.43_7(\pm0.01)$	0	$0.65_5(\pm0.01)$
2	0.0007	0.43_7	0.0062	0.65_1
4	0.0056	0.43_4	0.050	0.63_1
6	0.0192	0.43_0	0.16_8	0.59_3
8	0.045_0	0.42_4	0.40_0	0.52_2
10	0.088	0.41_0	0.45	0.24_1
12	0.152	0.39_2	0.40	0.10
14	0.242	0.36^6	0.12	0.016
16	0.32	0.29	(−)0.40	(−)0.029
18	0.18	0.10_0	(−)1.25	(−)0.060
20	(−)0.25	$(-)0.09_7$	(−)2.40	(−)0.082
22	(−)0.65	$(-)0.17_2$	(−)3.75	(−)0.096
24	(−)1.24	$(-)0.22_3$	(−)4.70	(−)0.096
26	(−)1.90	$(-)0.25_0$	(−)5.40	(−)0.089
28	(−)2.68	$(-)0.26_0$	(−)5.95	(−)0.082
30	(−)3.60	$(-)0.26_6$	(−)6.40	(−)0.075
32	(−)4.75	$(-)0.28_5$	(−)6.50	(−)0.067
34			(−)6.15	(−)0.057

[a] $\alpha=(0.880\pm0.016)\times10^{-12}T^3$, $T<15.5$°K.
[b] $\alpha=(7.80\pm0.15)\times10^{-12}T^3$, $T<12$°K.

Our original Ge sample was cut into two pieces (13.46 and 6.99 cm) to provide a systematic check of our need for end corrections, etc. The second sample holder also was used. The general agreement between the long-sample (open circle) and normalized short-sample (crosses) data is well within the experimental scatter. The scatter in these data at low temperatures (of the order of ±0.03 Å) is sufficiently small to establish unambiguously the T^4 length dependence even at temperatures below 6°K (see the $\Delta L\times10$ curve in Fig. 3).

2. GaAs and GaSb

The behavior of these two substances (Figs. 5 and 6) is quantitatively similar. The GaAs sample was removed from the sample holder and then remounted between runs 1 and 2. The agreement is good, showing again the independence of the results on handling and mounting of the sample.

3. InAs and InSb

The total positive expansions which were measured for these samples upon warming from 1.89°K to approximately 4°K, are the smallest that we have seen, being 0.7 and 0.5 Å, respectively. The data are sufficiently precise, however, to establish the T^4 dependence of the length. The low-temperature InAs data were obtained over a period of several days, and one measurement was made with the liquid helium at 1.2°K to assist in the extrapolation to absolute zero. The extrapolation of the InSb data to absolute zero was made by means of a fit of the data from 1.89 to 3.2°K. The thermal-expansion coefficients for InSb as given by Gibbons[1] are indicated on Fig. 8 also. The agreement is qualitative and within the precision of his interferometric technique.

B. Grüneisen Constants

The thermal-expansion data for these six related cubic solids are compared best by a calculation of the temperature dependence of their Grüneisen parameters $\gamma(T)$. In the following γ is defined as

$$\gamma=\frac{3\alpha B_T V}{C_V}=\frac{\sum\gamma_i c_i}{\sum c_i}, \qquad (1)$$

where C_V/V is the heat capacity at constant volume per unit volume, α is the linear-thermal-expansion coefficient, and $B_T=-V(\partial P/\partial V)_T$ is the isothermal bulk modulus. The temperature dependence of both B_T and V is small in our temperature range (0 to 40°K) so can be ignored. C_V, however, varies rapidly with temperature and either must be known from experimental data or must be estimated on the basis of a model.

The right-hand term of Eq. (1) gives the microscopic significance of this definition of γ in the quasiharmonic approximation. Here, c_i is the magnitude of constant-

TABLE III. Smoothed values for the linear-thermal-expansion coefficient α and the Grüneisen constant γ for GaAs, GaSb, InAs, and InSb.

T (°K)	GaAs[a] α (10^{-8} °K^{-1})	GaAs[a] γ	GaSb[b] α (10^{-8} °K^{-1})	GaSb[b] γ	InAs[c] α (10^{-8} °K^{-1})	InAs[c] γ	InSb[d] α (10^{-8} °K^{-1})	InSb[d] γ
0	0	0.583(±0.01)	0	0.297(±0.01)	0	0.285(±0.01)	0	0.21(±0.01)
2	0.0069	0.583	0.0084	0.286	0.011	0.28	0.013	0.20
4	0.055	0.569	0.067	0.256	0.025	0.066	0	0
6	0.187	0.535	0.226	0.202	(−)0.25	(−)0.145	(−)1.5	(−)0.41
8	0.445	0.472	(−)0.1	(−)0.03	(−)1.6	(−)0.30	(−)9.4	(−)0.80
10	0.45	0.202	(−)2.6	(−)0.27	(−)5.8	(−)0.43	(−)24.0	(−)0.93
12	0.10	0.02	(−)7.0	(−)0.40	(−)12.5	(−)0.52	(−)43.2	(−)0.95
14	(−)0.95	(−)0.114	(−)12.5	(−)0.441	(−)22.0	(−)0.59	(−)65.0	(−)0.95
16	(−)2.75	(−)0.182	(−)18.3	(−)0.441	(−)0.335	(−)0.615	(−)87.0	(−)0.95
18	(−)4.9	(−)0.223	(−)24.2	(−)0.421	(−)45.	(−)0.63	(−)108	(−)0.95
20	(−)7.5	(−)0.239	(−)29.0	(−)0.392	(−)55.5	(−)0.62	(−)123	(−)0.925
22	(−)10.0	(−)0.241	(−)32.3	(−)0.357	(−)65.	(−)0.61	(−)134	(−)0.90
24	(−)12.5	(−)0.238	(−)33.8	(−)0.318	(−)73	(−)0.60	(−)142	(−)0.84
26	(−)14.4	(−)0.226	(−)34.2	(−)0.279	(−)79	(−)0.56	(−)143	(−)0.77
28	(−)16.2	(−)0.215	(−)33.5	(−)0.239	(−)835	(−)0.53	(−)141	(−)0.69
30	(−)17.7	(−)0.20	(−)31.5	(−)0.208	(−)86	(−)0.50	(−)135	(−)0.61
32	(−)17.7	(−)0.177	(−)28.5	(−)0.167	(−)875	(−)0.47	(−)126	(−)0.53
34	(−)16.7	(−)0.149			(−)885	(−)0.44	(−)117	(−)0.46
36	(−)15.1	(−)0.12			(−)885	(−)0.41		
38	(−)12.7	(−)0.09			(−)865	(−)0.375		
40	(−)10.5	(−)0.065			(−)825	(−)0.34		
42					(−)785	(−)0.305		

[a] $\alpha = (8.68 \pm 0.16) \times 10^{-12} T^3$, $T < 8.0$°K.
[b] $\alpha = (10.5 \pm 0.2) \times 10^{-12} T^3$, $T < 6.7$°K.
[c] $\alpha = (13.6 \pm 0.7) \times 10^{-12} T^3$, $T < 3.5$°K.
[d] $\alpha = (16 \pm 1) \times 10^{-12} T^3$, $T < 3.3$°K.

volume heat-capacity contribution associated with a lattice frequency mode ν_i, and $\gamma_i = -(d \ln \nu_i / d \ln V)$. "Normal" behavior involves positive γ_i's and positive thermal expansion. In the elastic continuum model, the shapes of the dispersion relations for the various branches of the lattice frequency spectrum are not a function of volume; i.e., the γ_i's for all the frequencies in that branch (transverse acoustic, longitudinal acoustic, etc.) are the same although usually different for different branches. In the more general case, the γ_i's are a function of frequency for all branches, and the shapes of the various dispersion relations are a function of volume. This latter case applies to the solids considered in this paper.[5,8]

The existing low-temperature heat-capacity data for Ge and Si show large deviations from a Debye-type behavior,[23,24] as is shown by the reduced Θ-versus-T curves of Fig. 9. Here Θ_0 is the extrapolated value of Θ at absolute zero, and Θ is the characteristic temperature calculated from the observed specific heat, the actual experimental temperature, and the Debye function. The expected low-temperature T^3 dependence of C_V occurs (to 1% precision) only for reduced temperatures $T/\Theta_0 < 0.006$. The actual experimental data for Ge and Si are sufficiently complete and precise so that we have used them directly in our calculations of γ.[23,24]

This is not true for the compounds, however, and we have used the reduced curves for Ge and Si in Fig. 9 as a guide for the extrapolation to low temperatures of higher-temperature data for these (from 12°K for GaAs, GaSb, and InAs[25] and from 6°K for InSb).[25,26] The reported data for InSb show considerable deviation above 20°K, but since Piesbergen's results are in good

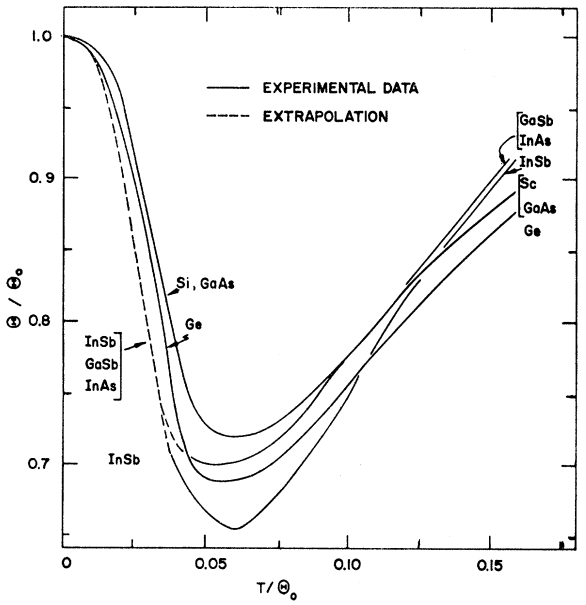

FIG. 9. Reduced Θ-versus-T curves for the six solids studied in this work. The sources of these curves are discussed in the text.

[23] P. Flubacher, A. J. Leadbetter, and J. A. Morrison, Phil. Mag. 4, 273 (1959).
[24] C. A. Bryant and P. H. Keesom, Phys. Rev. 124, 698 (1961).
[25] U. Piesbergen, Z. Naturforsch. 18a, 141 (1963).
[26] Y. Ohmura, J. Phys. Soc. Japan 20, 350 (1965).

TABLE IV. Assumed $T=0$ values of parameters used to calculate γ. Atomic volumes are those used for the elastic-constant determinations.

	Si	Ge	GaAs	GaSb	InAs	InSb
Θ_0(°K)	645[a]	374[a]	345[b]	266[c]	234[d]	205[e]
B_T(kbar $=10^9$ dyn/cm^2)	995[f]	765[g]	789[b]	570[h]	634	483[e]
V(cm^3/g atom)	12.06[f]	13.59[g]	13.58[b]	17.1[h]	16.7[d]	20.45[e]

[a] Flubacher *et al.* (Ref. 23) (calorimetric).
[b] Garland and Park (Ref. 27) (4°K).
[c] Calculated by Piesbergen (Ref. 31) from 300°K data.
[d] Gerlich (Ref. 28) (4°K).
[e] Slutsky and Garland (Ref. 29) (4°K).
[f] McSkimmin and Andreatch (Ref. 36) (77°K).
[g] McSkimmin and Andreatch (Ref. 37) (77°K).
[h] Einspruch and Manning (Ref. 30) (300°K).

agreement with other data for Ge, we have accepted his data[25] for InSb at high temperatures.

In the absence of calorimetric data, values of Θ_0 can be calculated from low-temperature ultrasonic measurements of elastic constants. The agreement between calculated elastic-constant values of Θ_0 and the calorimetric values is excellent for Ge and Si.[23] Liquid-helium-temperature data exist for the elastic constants of GaAs,[27] InAs,[28] and InSb[29] while the only measurements for GaSb are for room temperature.[30] The values of B_T, V, and Θ_0 given in Table IV are essentially those reported (or quoted) in the papers describing the ultrasonic work. The only exception is for the case of GaSb where we have used a calculated value quoted by Piesbergen.[31] The 4°K data[28] for InAs are considerably different from earlier 77°K data,[32] and the calculated Θ_0's differ considerably (234 versus 250°K). We have used the low-temperature values.

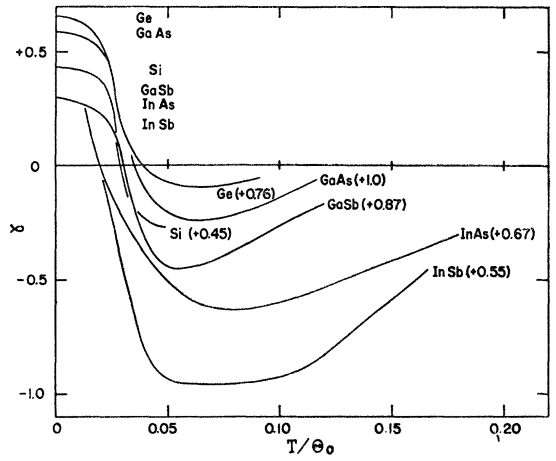

FIG. 10. The Grüneisen parameters for the various solids as a function of reduced temperature (Θ_0 is given in Table IV). The numbers in parentheses on the right-hand side are estimated room-temperature values of γ which are given to emphasize that all of these solids behave "normally" at room temperature.

The shapes of the reduced Θ-versus-T curves given in Fig. 9 were used together with the Θ_0, B_T, and V data in Table IV to calculate $\gamma(T)$ for each substance from the smoothed α data. The results of these calculations are given in the second column of Tables II and III. Figure 10 is a plot of these values of γ as a function of reduced temperature T/Θ_0. The numbers in parentheses are room-temperature γ's which are estimated from data given by Piesbergen.[25] These are included to emphasize that at room temperature the expansion coefficients of all of these solids are positive.

The uncertainties in the γ values for Ge and Si are due primarily to our thermal-expansion measurements (2 to 3%) since very reliable data exist for all of the other quantities in Eq. (1). The major uncertainties in the γ values for the other solids involve, at low temperature, the Θ_0 values used (since $\gamma_0 \sim \Theta^{-3}$) and, at higher temperatures, the interpolation procedure used to obtain values for C_V. The actual shapes of the curves plotted in Fig. 10 will not be affected appreciably by the use of direct heat-capacity data, but any detailed analysis of the results in the region where both γ and Θ are changing rapidly with temperature must wait for additional specific-heat results.

IV. DISCUSSION

The basic results of this series of measurements are summarized in the γ values given in Tables II and III and plotted in Fig. 10. The various curves for γ are qualitatively similar and differ only in detail. In particular, the thermal-expansion-coefficient data exhibit a T^3 dependence to a much higher relative temperature ($T/\Theta \sim 0.02$) than do the specific-heat data ($T/\Theta \sim 0.006$). This results in a general decrease in γ with increasing temperature at low temperature, paralleling the decrease in Θ observed in Fig. 9.

The curves in Fig. 10 show a systematic variation in shape (and magnitude) which, with the exception of Si, appears to be correlated with the Debye temperature of the solid. This correlation is illustrated in Fig. 11 where two features of these curves (the minimum and absolute-zero values of γ) are plotted as a function of Θ_0. As was mentioned above, the data for Si do not follow this correlation. Data for α—Sn ($\Theta \sim 230$°K) would be useful to complete our data for the III–V compounds in the 4th and 5th rows of the periodic

[27] C. W. Garland and K. C. Park, J. Appl. Phys. 33, 759 (1962).
[28] D. Gerlich, J. Appl. Phys. 35, 3062 (1964).
[29] L. J. Slutsky and C. W. Garland, Phys. Rev. 113, 167 (1959).
[30] N. G. Einspruch and R. J. Manning, J. Acoust. Soc. Am. 35, 215 (1963).
[31] U. Piesbergen, in *Physics of III-V Compounds*, edited by R. K. Willardson and A. C. Beer (Academic Press Inc., New York, 1966), Vol. 2, p. 49.
[32] D. Gerlich, J. Appl. Phys. 34, 2915 (1963).

table, and data for AlP ($\Theta\sim580$°K) would be of interest to compare with those for Si. Novikova's data[2] suggest that II–VI compounds behave similarly to the III–V compounds at high temperatures, and if indeed CdTe fits into the "picture" of Fig. 10, its value of Θ (140°K) should be sufficiently low to reduce its initial positive expansion region to zero. At higher Θ values, AlAs ($\Theta\sim420$°K) might show only a very limited region of negative expansion coefficient.

The basic reason for the complicated temperature dependence of these related tetrahedrally-bonded compounds is not understood. As was mentioned in the Introduction, the possibility exists that this behavior is characteristic of all tetrahedrally bonded solids. The existence of the very low temperature positive-expansion region was postulated by Daniels[5] from considerations based on third-order elastic-constant data. Inelastic neutron diffraction data show that the lowest-lying (transverse acoustic) dispersion curve for Ge and Si (as well as for diamond and GaAs)[8] bends over sharply and becomes almost horizontal for low k values. This behavior is responsible for the rapid decrease in Θ with increasing temperature shown in Fig. 9. Daniels suggested that the low-temperature positive expansion region was due to a normal (positive mode γ) behavior for the initial (low-frequency) portion of this curve while the rapid decrease in expansion at slightly higher temperatures was due to an abnormal behavior (negative mode γ) at the higher frequencies. The first of these is shown by the third-order elastic-constant data while the second behavior has been shown in measurements of the pressure dependence of phonon-assisted interband tunneling in the 111 direction in Sb-doped germanium.[33] At high temperatures, the normal behavior of the other modes causes a return to positive-thermal-expansion behavior. Bienenstock[34] was able to fit the thermal-expansion data for Ge using an *ad hoc* type of calculation with one adjustable constant. This constant has no easily identifiable physical significance, however.

Daniel's original calculations of γ_0 for Si and Ge were confirmed by Collins[35] who also discusses the inadequacy of the "anisotropic continuum model" as applied to Ge and Si. The original thermal-expansion data of Carr *et al.*[7] agree qualitatively with the γ_0's predicted by Daniels and Collins. Our more precise thermal-expansion data give values of γ_0 (Table II) which, while positive, are considerably larger than can be calculated from the most recent, 77°K, high-pressure elastic-constant data for Si[36] and Ge.[37] The comparison between the elastic-constant values γ_0^{el} and the present thermodynamic values γ_0^{el} and the present thermodynamic values γ_0^{th} is given in the first two columns of Table V. The calculations from the elastic-constant data are most sensitive to the value of dC_{44}/dP,[5] and the use of the 77°K rather than the 300°K high-pressure data has served to accentuate the difference between the elastic and thermodynamic values of γ_0. Both C_{44} and dC_{44}/dP have changed by such small amounts from 300 to 77°K that it is difficult to picture radical changes in the magnitude of dC_{44}/dP upon further cooling to 4°K. A further complication is introduced by the excellent agreement between the calorimetric and elastic-constant values of Θ_0 for Ge and Si,[23] the implication being that the lattice-continuum model applies in this case.

Third-order elastic-constant data recently have been published for GaAs.[38,39] The data of Drabble and Brammer,[38] although for room temperature, can be used to estimate a value of γ_0 of approximately 0.6, which is in excellent agreement with the thermal value of 0.58. The data of McSkimmin and Andreatch,[39] however, resemble very closely those for Ge, and will give a value of γ_0 which is roughly $\frac{2}{3}$ of the thermal value. The reason for the discrepancy in these third-order elastic-constant data is not known.

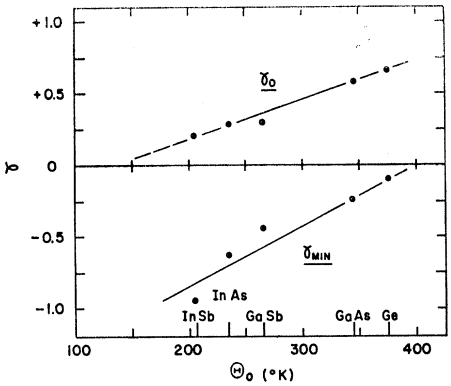

FIG. 11. The dependence on Θ_0 of two of the features of the curves shown in Fig. 10. γ_0 is the absolute zero value, γ_{min} is the minimum value of γ. The data for Si are not included.

TABLE V. A comparison of the experimental and calculated values of the Grüneisen parameter defined by Eq. (1).

	γ_0^{th} [a]	γ_0^{el} [b]	γ_0^{sh} [c]
Si	0.44	0.21	(0.39)
Ge	0.66	0.47	(0.62)

[a] Table II.
[b] Calculated by J. G. Collins from the data in Refs. 36 and 37 (private communication).
[c] Estimated by R. A. Cowley from the model of Ref. 8 (private communication).

[33] H. Fritzsche, in *Physics of Solids at High Pressures*, edited by C. T. Tomizuka and R. M. Emrick (Academic Press Inc., New York, 1965), p. 184.
[34] A. Bienenstock, Phil. Mag. **9**, 755 (1964).
[35] J. G. Collins, Phil. Mag. **8**, 323 (1963).
[36] H. J. McSkimmin and P. Andreatch, Jr., J. Appl. Phys. **35**, 2161 (1964).
[37] H. J. McSkimmin and P. Andreatch, Jr., J. Appl. Phys. **34**, 651 (1963).
[38] J. R. Drabble and A. J. Brammer, Solid State Commun. **4**, 467 (1966).
[39] H. J. McSkimmin and P. Andreatch, Jr., J. Appl. Phys. **38**, 2362 (1967).

Dolling and Cowley recently have succeeded in fitting the inelastic neutron scattering dispersion relationships for diamond, Si, Ge, and GaAs with a shell-model calculation.[8] They have been able to reproduce the observed Θ-versus-T relations for these solids, and by means of two adjustable parameters which reflect the volume dependence of two of the shell-model parameters, they have been able to reproduce the higher-temperature thermal-expansion behavior. The qualitative change in shape of the lowest transverse-acoustic dispersion relation with decreasing volume is confirmed, and a discrepancy with respect to the high-pressure elastic-constant measurements for this mode is reported. They do not give a value of γ_0 since the grid of points which they used was not sufficiently fine to give a reliable value. Approximate values of γ_0 can be calculated within these limitations, however, which are surprisingly close to the values which we observe (Table V).[40] No basis for a discrepancy between γ_0^{th} and γ_0^{el} exists in the theory.

Note added in proof. Dr. D. E. Schuele of the Case Institute of Technology has used the high-pressure elastic-constant data given in Refs. 36, 37, and 39, and a computer program which uses 184 equally spaced points over the unit triangle of a cubic crystal [J. Phys. Chem. Solids **25**, 801 (1964)] to calculate γ_0's for Si, Ge, and GaAs. The γ_0's calculated for the 77°K Si and Ge data (0.211 and 0.480, respectively) agree with those given in Table V. The γ_0 calculated for the room-temperature GaAs data (0.367) perhaps should be reduced by from 5 to 10% (by analogy with Ge) to obtain a true absolute zero value. The resulting estimate of 0.35 is to be compared with our thermal value of 0.58 (Table III). The authors are indebted to Dr. Schuele for carrying out these calculations.

[40] R. A. Cowley (private communication).

PHYSICAL REVIEW VOLUME 163, NUMBER 3 15 NOVEMBER 1967

Electrical Studies of Electron-Irradiated *n*-Type Si: Impurity and Irradiation-Temperature Dependence*

HERMAN J. STEIN AND FREDERICK L. VOOK
Sandia Laboratory, Albuquerque, New Mexico
(Received 3 May 1967)

Electrical-conductivity and Hall-coefficient measurements have been used to investigate the crystal growth and irradiation-temperature dependence of the introduction and annealing of defects in electron-irradiated *n*-type silicon. Irradiations of 10-Ω cm, phosphorus-doped silicon with 1.7-MeV electrons were performed at controlled temperatures between 75 and 300°K, and isochronal annealing was investigated between 80 and 700°K. Both intrinsic defects and impurity-associated defects are observed. The impurity independence of annealing between 100 and 200°K suggests the annealing of intrinsic defects. The introduction rate for these intrinsic defects is independent of the irradiation temperature between 75 and 100°K. The introduction rates for the impurity-associated defects, however, exhibit an exponential dependence on the reciprocal irradiation temperature between 75 and 100°K consistent with a model based on metastable vancacy-interstitial pairs that predicts a temperature-dependent probability for vacancy-interstitial dissociation during irradiation and subsequent trapping by crystal impurities. For irradiations above 100°K, the introduction rates of impurity-associated defects are relatively independent of the irradiation temperature. Excluding the carrier-removal annealing which is associated with the intrinsic-defect stage, 90% of the annealing in crucible-grown silicon and ~70% of the annealing in float-zone, Dash, and Lopex silicon correlate with the annealing of the divacancy and impurity-associated defects observed in EPR and optical-absorption studies on *n*-type silicon. In crucible-grown silicon, the annealing temperatures of the dominant electrically active, impurity-associated defects correlate with those for the *A* center and other oxygen-associated defects. Measurements of carrier concentration versus temperature provide additional evidence for the dominance of the *A* center which has an energy level near $E_c-0.185$ eV, where E_c is the energy of the conduction-band minimum. A level near $E_c-0.13$ eV also is observed in crucible-grown silicon for the oxygen-associated defects responsible for reverse annealing between 200 and 250°K. In float-zone silicon, the annealing temperatures of the dominant electrically active defects correlate with the *E*-center and divacancy annealing. Lopex silicon is very similar to Dash silicon, and in these materials all the annealing stages of crucible and float-zone silicon are observed.

I. INTRODUCTION

INTRINSIC structural defects such as vacancies and interstitials are produced in silicon crystals by high-energy particle irradiation. Significant thermal reordering and impurity trapping of these defects occur below room temperature so that electrically active impurity-associated defect complexes are observed following irradiation at temperatures where the intrinsic defects are mobile.[1] To understand radiation effects in silicon,

* This work supported by the U. S. Atomic Energy Commission.

[1] For a recent review of radiation-induced defects in silicon, see J. W. Corbett, in *Solid State Physics*, edited by F. Seitz and D. Turnbull (Academic Press Inc., New York, 1966), Suppl. 7, p. 59.